



**HAL**  
open science

## Determination of the microplastic content in Mediterranean benthic macrofauna by pyrolysis-gas chromatography-tandem mass spectrometry

Magali Albignac, Jean François Ghiglione, Céline Labrune, Alexandra ter Halle

► **To cite this version:**

Magali Albignac, Jean François Ghiglione, Céline Labrune, Alexandra ter Halle. Determination of the microplastic content in Mediterranean benthic macrofauna by pyrolysis-gas chromatography-tandem mass spectrometry. *Marine Pollution Bulletin*, 2022, 181, pp.113882. 10.1016/j.marpolbul.2022.113882 . hal-03773577

**HAL Id: hal-03773577**

**<https://hal.science/hal-03773577v1>**

Submitted on 12 Oct 2023

**HAL** is a multi-disciplinary open access archive for the deposit and dissemination of scientific research documents, whether they are published or not. The documents may come from teaching and research institutions in France or abroad, or from public or private research centers.

L'archive ouverte pluridisciplinaire **HAL**, est destinée au dépôt et à la diffusion de documents scientifiques de niveau recherche, publiés ou non, émanant des établissements d'enseignement et de recherche français ou étrangers, des laboratoires publics ou privés.

1 Determination of the microplastic content in Mediterranean benthic  
2 macrofauna by pyrolysis-gas chromatography-tandem mass  
3 spectrometry

4  
5 Magali Albignac<sup>1</sup>, Jean François Ghiglione<sup>2</sup>, Céline Labrune<sup>3</sup>, Alexandra ter Halle<sup>1\*</sup>

6  
7 <sup>1</sup>CNRS, Université de Toulouse, Laboratoire des Interactions Moléculaires et Réactivité Chimique  
8 et Photochimique (IMRCP), UMR 5623, Toulouse, France

9 <sup>2</sup>CNRS, Sorbonne Université, Laboratoire d'Océanographie Microbienne (LOMIC), UMR 7621,  
10 Observatoire Océanologique de Banyuls, Banyuls sur mer, France

11 <sup>3</sup>CNRS, Sorbonne Université, Laboratoire d'Ecogéochimie des Environnements Benthiques  
12 (LECOB), UMR 8222, Observatoire Océanologique de Banyuls, Banyuls sur mer, France

13  
14 \*Corresponding author:

15 Alexandra ter Halle Laboratoire des Interactions Moléculaires et Réactivité Chimique et  
16 Photochimique (IMRCP), UMR 5623, 31062 Toulouse Cedex 9, France. Tel.: + 33 (0)561558457.

17 E-mail address: [ter-halle@chimie.ups-tlse.fr](mailto:ter-halle@chimie.ups-tlse.fr)

18  
19  
20 **Abstract**

21 The Mediterranean Sea water bodies are ones of the most polluted, especially with  
22 microplastics. As the seafloor is the ultimate sink for litter, it is considered a hotspot for  
23 microplastic pollution. We provide an original analytical development based on the  
24 coupling of tandem mass spectrometry to pyrolysis-gas chromatography to improve the  
25 detection of plastic contamination in marine organisms. Due to the high selectivity of the  
26 mass spectrometer, a straightforward sample preparation consists uniquely of potassium  
27 hydroxide digestion. The quantification of six common polymers is possible in one run.  
28 The method was applied to analyze the plastic content from 500 µm down to 0.7 µm in the  
29 whole body of seven benthic species with variable feeding modes. Plastic was detected in

30 all samples, with an almost systematic detection of polypropylene and polyethylene. Our  
31 method presents a major development in determining the levels of plastic contaminations  
32 in samples with rich organic matter content.

33

### 34 **Keywords**

35 Plastic pollution, marine litter, polymer, bioaccumulation, biodiversity, ingestion, benthic  
36 macrofauna

37

### 38 **Highlights**

39

40 • A method for quantifying microplastics in marine organisms down to 0.7  $\mu\text{m}$  was  
41 developed using pyrolysis coupled to tandem gas chromatography–mass spectrometry.

42 • A one-step sample preparation consisting of chemical digestion was utilized.

43 • Six distinct polymer contents were determined in one run.

44 • The total polymer contents varied greatly from one organism to the other and was between  
45 105 and 7780  $\mu\text{g/g dw}$ .

46 • The PE, PET and PS polymers were detected the most often.

47

### 48 **Introduction**

49

50 Plastic loads are increasing in marine ecosystems worldwide (Barnes et al. 2009),  
51 and the Mediterranean Sea is one of the most affected marine basins (Consoli et al., 2020;  
52 (Galgani et al., 1996). Macrolitter densities that exceeded  $10^5$  items per  $\text{km}^2$  were recorded  
53 near metropolises (Galgani et al., 2000). Microplastic concentrations (less than 5 mm) on the  
54 seafloor, which are considered hotspots of accumulation, can reach up to 1.9 million pieces  
55 per  $\text{m}^2$  (Kane et al., 2020).

56 An initial explanation for microplastic littering is that the litter is transported to the  
57 seafloor by vertical settling from surface accumulations and is driven by the density of  
58 microplastics. With biofouling, the buoyancy of microplastics is altered, and all types of  
59 plastic can sink—whether they are initially buoyant or not (Kooi et al., 2017). Whereas  
60 macrolitter sinking may be associated with dense downcanyon flows in the Mediterranean

61 (de Madron et al., 2017; Tubau et al., 2015), microplastic sedimentation in the deep sea is  
62 driven more by near-bed thermohaline currents (Kane et al., 2020). In coastal areas,  
63 seasonal changes in river flow rate and related turbidity currents also considerably impact  
64 the spatial dispersion of litter (Angiolillo et al., 2021).

65 Microplastic hotspots are also likely hotspots for marine life, as has been shown  
66 from the sea surface microlayer (Ghiglione and Laudet, 2020) to deep-sea sediment (Hall,  
67 2002; Kane et al., 2020). Marine biota interact with microplastics in several ways, and this  
68 leads to a reduction in feeding and depletion in energy stores but also causes toxicity,  
69 carcinogenesis, endocrine disruption and physical harm with knock-on effects for fecundity  
70 and growth (Galloway et al., 2017). After sedimentation, microplastics are available for  
71 many benthic species to feed on, such as detritivores and filter-feeding species (Valente et  
72 al., 2020). This potentially impacts the biodiversity throughout marine life, as the benthic  
73 community plays an important role in providing resources and ecosystem services  
74 (Danovaro et al., 2020; Manea et al., 2020). The extent of the impacts of plastic pollution  
75 on Mediterranean ecosystems is poorly estimated, whereas the Mediterranean Sea is a  
76 biodiversity hotspot with high levels of endemism (Coll et al., 2010). Monitoring litter-  
77 benthic community interactions is largely hampered by difficulties in sampling and the  
78 necessary costs (Angiolillo et al., 2021; Valente et al., 2020), which is why the interactions  
79 are poorly described even if all reported studies declare that a quasi-systematic of plastic  
80 occurs in individuals (Anastasopoulou et al., 2013).

81 In general, microplastics that are larger than 500  $\mu\text{m}$  are visually detected and  
82 identified by Fourier Transform Infrared Spectroscopy (FT-IR). There are very few  
83 publications that compare microplastics that are smaller than 150  $\mu\text{m}$ . The latest  
84 spectroscopic developments allow limits of tens of microns to be reached (Schwaferts et  
85 al., 2019), but the detection of the particles is strongly impacted by residual organic matter.  
86 This is solved by intensive sample preparations, which are time-consuming and costly  
87 forms of analysis that involve risks including altering and losing some microplastics and  
88 increasing cross contamination. In this context, pyrolysis-gas chromatography–mass  
89 spectrometry (Py-GC–MS) appears to be a very promising technique, even if its  
90 developments are very recent (Yakovenko et al., 2020). The use of Py-GC–MS does not  
91 have size limitations, and the selectivity of the mass spectrometry offers the possibility to  
92 simplify the sample preparation. The use of Py-GC–MS is promising in terms of reducing  
93 the time of analysis because several polymers are detected in one run.

94 In addition to all these promising aspects, there are some consequent obstacles with  
95 the use of Py-GC-MS (Pico and Barcelo, 2020; (Yakovenko et al., 2020). Two recent  
96 studies with important developments resulted, for the first time, in achieving the following  
97 robust methods: one for the analysis of biosolids (Okoffo et al., 2020) and the other for  
98 seafood samples (Ribeiro et al., 2020). Even if a less intensified purification of the sample  
99 is obtained through the use of Py-GC-MS, this step is still important. Okoffo et al. (2020)  
100 opted for pressurized liquid extraction, and the remaining organic matter was eliminated  
101 during Py-GC-MS analysis using a two-step pyrolysis program (organic matter removal at  
102 300 °C followed by pyrolysis at 650 °C). Ribeiro et al. (2020) proposed a more intensified  
103 sample purification that involved alkaline digestion followed by pressurized liquid  
104 extraction, and they skipped the decomposition step at 300 °C. Here, we introduce the use  
105 of tandem mass spectrometry (Py-GC-MS/MS) to enhance the detection performance, thus  
106 permitting a simpler sample preparation using alkaline digestion alone. This study aimed  
107 to demonstrate that Py-GC-MS/MS is a fast and reliable tool for microplastic  
108 quantification down to 0.7 µm in marine organisms. Here, we provide the first assessment  
109 of microplastic content in Mediterranean benthic organisms for a selection of 6 different  
110 polymers.

111

## 112 **2. Materials and Methods**

### 113 **2.1. Chemicals and Reference Materials.**

114 A total of six polymers were targeted. They were chosen among the most abundant  
115 polymers in the marine environment, namely, high density polyethylene (PE), poly(methyl  
116 methacrylate) (PMMA), polyethylene terephthalate (PET), polycarbonate (PC),  
117 polystyrene (PS), and polypropylene (PP). The first three polymers were purchased from  
118 Sigma-Aldrich (St. Louis, MO, USA) and the three others were from Goodfellow Group  
119 (Huntingdon, United Kingdom). These polymer standards were used to optimize the mass  
120 spectrometry conditions and to prepare standards for external calibration. The external  
121 calibration was performed with a mix of polymers diluted in a calcined powdered glass  
122 microfiber filter (GF/D diameter 47 mm; Whatman® Sigma-Aldrich, St. Louis, MO,  
123 USA).

124

125

126 **2.2. Sample Collection and Processing.**

127 All glassware was calcined at 550 °C for 2 hours before use in an incinerator oven  
128 (Nabertherm™ LV052K1RN1). Glass fiber filters were calcined at 600 °C for 2 hours  
129 before use. Benthic organisms were sampled on the northwestern Mediterranean seafloor  
130 from the R/V Nereis II. Specimens sampled with a van veen grab were sorted and stored  
131 in a clean metallic bowl on board. At the laboratory, the specimen were identified and  
132 placed in calcined glass vials that were closed with a cap, which was equipped with a  
133 polytetrafluoroethylene (PTFE) opercula. The details of the GPS location and sampling  
134 depth of each organism are given in Table 1. A sampling control consisted of opening a  
135 calcined glass vial that contained calcined quartz fiber for approximately the same period  
136 of time it took to manipulate the animals both onboard and at the laboratory. The quartz  
137 fiber was analyzed by Py-GC–MS/MS similar to the samples. In the laboratory, all animals  
138 were freeze-dried and weighed. Under the hood, the animals were transferred to 30 mL  
139 glass flasks equipped with glass caps. A ratio of 80 mL per gram of dry animal of 10%  
140 potassium hydroxide aqueous solution prefiltered was added. The solution was previously  
141 filtered in a closed glass unit from Vagner Glasses Company (Toulouse) on a calcined 47  
142 mm diameter membrane with a porosity of 0.45 µm (PTFE Omnipore™, from Sigma–  
143 Aldrich, St. Louis, MO, USA) to remove any potential plastic contamination. For the  
144 chemical digestion, the flasks were placed in a shaker incubator (Eppendorf®  
145 ThermoMixer® C, Sigma–Aldrich, St. Louis, MO, USA) for 48 h at 40 °C with continuous  
146 agitation (500 rpm). A similar flask with potassium hydroxide solution and no sample was  
147 used as a procedural blank. Once the digestion was completed, the samples were removed  
148 from the incubator and prefiltered on 500 µm stainless steel filter grids (Negofiltre, Moret  
149 Loing Et Orvanne, France). The solution was then filtered under vacuum with a closed  
150 glass unit onto a calcined glass microfiber filter, GF/F diameter 47 mm or 21 mm  
151 Whatman® (Sigma–Aldrich, St. Louis, MO, USA). Filters were stored in glass Petri dishes  
152 before cryogrinding using the SPEX® SamplePrep 6775 Freezer/Mill cryogenic Grinder  
153 (Delta Labo, Avignon) with the program: precool 2 min ; run 1min ; cool 2 min ; cycles  
154 15 ; cps 15. A sub-sample of 2 mg was precisely weighted in a microscale with a 10-5 g  
155 precision (Micro Balance from Sartorius, MCE225P-2S00-A Cubis®-II Semi) on quartz  
156 tubes that were freshly calcined at 1000°C with the pyrolysis probe using the “clean”  
157 program. A sub-sample of 2 mg was precisely weighted in a microscale with a 10-5 g  
158 precision (Micro Balance from Sartorius, MCE225P-2S00-A Cubis®-II Semi) on quartz

159 tubes that were freshly calcined at 1000°C with the pyrolysis probe using the “clean”  
 160 program.

161 **Table 1. List of the benthic organisms that were sampled in the northwestern**  
 162 **Mediterranean and analyzed for microplastic contents. The corresponding feeding**  
 163 **modes, sampling depths and coordinates are also given.**

164

<b>Taxa</b>	<b>Phylum</b>	<b>Feeding modes</b>	<b>Depth (m)</b>	<b>Coordinate s (WGS84)</b>
<i>Glandiceps talaboti</i>	Enteropneusta	Surface and/or Subsurface deposit feeder	43	42°30.50'N 3°09.11'E
<i>Amphiura chiajei</i>	Echinodermata	Surface deposit feeder	43	42°30.50'N 3°09.11'E
<i>Amphiura filiformis</i>	Echinodermata	Surface deposit and/or suspension feeder	43	42°30.50'N 3°09.11'E
<i>Notomastus sp.</i>	Annelida	Subsurface deposit feeder	43	42°30.50'N 3°09.11'E
<i>Fustiaria rubescens</i>	Molluska	Carnivorous	80	42°30.00'N 3°11.40'E
<i>Acanthocardia sp.</i>	Molluska	Suspension feeder	80	42°30.00'N 3°11.40'E
<i>Lanice conchilega</i>	Annelida	Surface deposit feeder and/or suspension feeder	90	42°30.00'N 3°12.60'E

165

166

### 167 **2.3 Py-GC–MS/MS Analysis.**

168 The method parameters for analysis by pyrolysis were achieved using a CDS Pyroprobe®  
 169 6150 from Quad service (Acheres, France) interfaced with a GC–MS/MS triple quadrupole  
 170 TSQ® 9000, GC Trace 1310 from Thermo Fisher Scientific (Villebon sur Yvette, France).  
 171 The gas chromatography column was a TraceGOLD TG-5SilMS from Thermo Fisher  
 172 Scientific. Samples were pyrolyzed at 600 °C for 30 s. The pyrolysis products were  
 173 transferred at 300 °C at the interface and were injected at 300 °C with a split ratio of 15:1  
 174 (additional data Table SI 1). Multiple reaction monitoring (MRM) optimizations for

175 collision energy were obtained using Auto SRM 4.0 for Chromeleon software in liquid  
176 injection with a Thermo Scientific™ AI/AS 1310 autosampler. The MS  
177 acquisition/detection parameters are listed in Table SI 2. Chromatograms were integrated  
178 using the Cobra detection algorithm from Chromeleon 7.2.8 software. The external  
179 calibrations were achieved between 25 ng and 1.4 µg with 6 calibration points (Table 2 and  
180 SI 3). The range of the calibration depends greatly on the polymer because the intensity of  
181 the indicator compound could vary greatly. The confirmation/quantification ratios were  
182 established with the external standards. For the external calibration preparation the  
183 polymers were first cryo-milled using the SPEX® SamplePrep 6775 Freezer/Mill cryogenic  
184 Grinder (Delta Labo, France) with the program: precool 2 min ; run 1 min ; cool 2 min ;  
185 cycles 15 ; cps 15. This inert matrix was prepared from glass microfiber filters (GF/D  
186 diameter 47 mm from Whatman®) cryo-milled (precool 1 min; run 1 min; cool 1 min;  
187 cycles 6; cps 15) and calcined.

188

## 189 **2.4 Method Validation and Performance**

190 For each polymer analyzed, an indicator compound was selected for quantification. The  
191 analytical limit of detection (LOD) and limit of quantification (LOQ) were determined for  
192 each polymer and were defined as S/N of 3 and of 10 respectively. This limit was only  
193 reached within the calibration range for PE (130 ng). We selected the following criteria to  
194 assess the possibility of determining a peak concentration: 1) the retention time was within  
195 a window of 0.05 min compared to that of the standards, 2) the peak was above the  
196 analytical LOQ, and 3) there was 30% tolerance in the ratio of the ion transitions. The  
197 interday variability will not be discussed as the external calibration standards and the samples  
198 were all analyzed in the same sequence on the same day. Finally, a polymer was quantified  
199 only if the signal was ten times superior to the procedural and field sampling blanks (Table  
200 SI 4) and we did not subtract the signal of the blank to the determined concentration. If any  
201 of the above cited criteria were not respected, it was specified that the concentration was  
202 not determined (n. d.). The extraction efficiency of the sample preparation was estimated  
203 with a positive control that consisted of the 6 polymers in concentrations ranging from 940  
204 to 4800 ng/ml of KOH and proceeded with the same steps as those of the preparation and  
205 analysis (Table SI 5). To evaluate matrix interferences during pyrolysis or mass  
206 spectrometry detection, we proceeded to perform the standard addition method after cryo-



207 grinding was performed for the filters, and the samples were spiked at concentrations of 50  
208 to 300 µg/g depending on the polymers.

## 209 **2.5. Quality Assurance and Quality Control (QA and QC)**

210 A need for stricter QA and QC during method development for microplastic analysis in  
211 biota was discussed earlier, and we integrated the criteria proposed in the present study  
212 (Hermsen et al., 2018). We took special care to minimize contamination during sampling  
213 and during sample preparation in the laboratory. Only glass and metal were used. The only  
214 plastic that was in contact with the sample was the opercula in the cap PTFE for sample  
215 storage, and this opercula is a polymer that does not interfere with the mass detection of  
216 the polymer targeted here. Glass and inox materials were cleaned thoroughly three times  
217 with Milli-Q water and ethanol and then systematically calcined prior to use. Laboratory  
218 coats that were made of 100% cotton were always worn during the analysis procedures.  
219 The work was performed in a fume hood to minimize contamination by airborne  
220 microplastics. Whenever the samples were not processed, they were stored in closed glass  
221 units. The glass fiber filters were also calcined and stored in glass petri dishes that were  
222 wrapped in aluminum foil before use. The quartz tubes that were used for access into the  
223 pyrolysis chamber were cleaned at 1000 °C for 30 s immediately before being used and  
224 were not stored. The samples in the quartz tube were weighed to minimize airborne  
225 contamination, as the tubes were placed in a metal sample holder that was stored in a glass  
226 unit with a glass cover. All solvents (water, ethanol, or potassium hydroxide solution) were  
227 prefiltered on PTFE (0.45 µm, Omnipore™, from Sigma–Aldrich, St. Louis, MO, USA).  
228 The glass microfiber filters were prepared via an optimized calcination (from room  
229 temperature to 500 °C at a rate of 80°C/hour with hold of 30 hours at 500°C using a LV  
230 5/11 furnace from Nabertherm®).

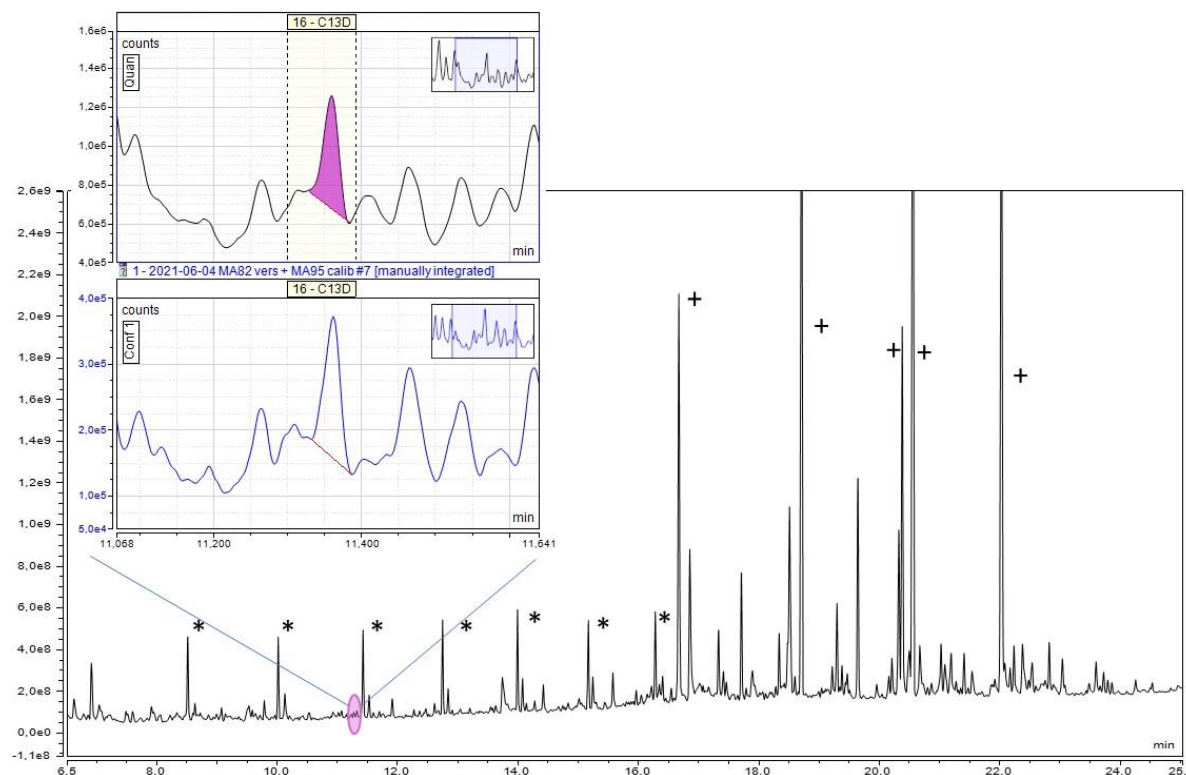
## 231 **3. Results and Discussion**

### 232 **3.1. Indicator compound detection and quantification**

233 The method proposed for the identification and quantification of the six targeted polymers  
234 (PMMA, PP, PE, PET, PS and PC) is new as it is the first development of tandem mass  
235 spectrometry coupled to pyrolysis. The high selectivity of the triple quadrupole allows to  
236 shorten the number of steps of the sampling preparation compared to what was proposed  
237 with a simple quadrupole (Ribeiro et al., 2020). Because PVC products of pyrolysis are  
238 aromatic molecules (like benzene, naphthalene ...) and because they are not specific (there  
239 are interferences from organic matter): we excluded this polymer from the study. For PS,

240 we selected the PS trimer as an indicator compound, as in most recent studies (Yakovenko  
241 et al., 2020). Styrene cannot be used because it is often a product of natural organic matter  
242 pyrolysis (Dierkes et al., 2019; (Fischer and Scholz-Bottcher, 2017; (Zhou et al., 2019).  
243 The specific detection of PE has already been discussed considerably because biogenic  
244 materials such as natural fats (e.g., fish protein) and waxes are rich in long alkyl chains.  
245 They produce n-alkanes and n-alkenes during pyrolysis (Dierkes et al., 2019; (Fischer and  
246 Scholz-Bottcher, 2017; (Scholz-Bottcher et al., 2013), which are common products in the  
247 pyrolytic decomposition of PE. The selection of an indicator compound among these two  
248 families was excluded if there was no intensive sample purification (Okoffo et al., 2020;  
249 (Ribeiro et al., 2020). Thus, we opted to use an indicator compound among the n-  
250 alkadienes, which are very specific to PE pyrolysis but formed to a much lesser extent  
251 (Yakovenko et al., 2020). In this study we selected the congener with 13 carbon atoms  
252 (Table 2). In the samples analyzed, we systematically detected PE in the MS/MS mode.  
253 The presence of PE was effective because all 3 congeners (the succession of n-alkadienes,  
254 n-alkene and n-alkane) were present with an n between 8 and 17. As a demonstration, we  
255 reported the signal in the full scan of one sample (Figure 1). The pyrochromatogram is very  
256 complex, but the characteristic shape of PE appears in the full scan with the n-alkenes  
257 signal (marked with a star in Figure 1). Some fatty acid esters were also present in important  
258 proportions and originated from residual organic tissues after chemical digestion. In the  
259 inset of Figure 1, the detection of the indicator compound, the n-alkadiene with 13 carbon  
260 atoms, is possible with the use of MS/MS. In this insert, we can see that in addition to the  
261 indicator compound, we detected many other peaks in MS/MS. Many peaks can be detected  
262 in MS/MS (MRM mode) because they have the same transitions as the ones monitored for  
263 the C13 target compound which is rather common among hydrocarbon derivatives but the  
264 transition ratios are distinct even for structural isomers. All those peaks are hydrocarbons  
265 with various unsaturated components and ramifications and are always formed during PE  
266 pyrolysis (Sojak et al., 2007). The interference of PE pyrolysis from organic matter,  
267 especially with regards of lipids, is a very complex problem which was recently  
268 investigated in details (Rauert et al., 2022). In the present study we have considered the  
269 ratio C13/C14 as a validation criterion with a tolerance of 30% compared to the ratios  
270 recorded for the external standards. Work is under progress to further understand PE  
271 pyrolysis and interferences with the matrix investigating several indicator compounds (the  
272 ratios recorded for the samples are presented in figure SI 1). In a recent review paper, we

273 argued for the choice of indicator compound selections for the other polymers (Yakovenko  
274 et al., 2020).



275  
276

277 Figure 1: Full scan analysis of the *Amphiura filiformis* sample. The stars mark the peaks of  
278 the n-alkene congeners; they are the main products of pyrolytic PE decomposition. The  
279 peaks marked with a cross are fatty acid esters and remains of the tissues of the animals  
280 after chemical digestion. In the inset box, the signal of the selected indicator compound of  
281 PE is presented in the MS/MS; we chose the alkadiene congener with 13 carbon atoms  
282 because its signal was the highest.

### 283 3.2 Sample digestion efficiency and evaluation of polymer integrity

284 We selected a chemical digestion protocol using potassium hydroxide to remove the  
285 organic tissues. The efficiency of this protocol was discussed considerably, and potassium  
286 hydroxide appeared to be a good compromise for obtaining an efficient purification and  
287 preserving the polymers (Dehaut et al., 2016). We observed that even if the organisms  
288 sampled were very distinct in terms of their taxonomic species, size, weight and feeding  
289 modes, the protocol was well adapted to this diversity. The digestion efficiency was  
290 estimated by mass balance; we determined that between 97 and 80% of the samples weight  
291 was eliminated. The elementary analysis of the remaining matter showed less than 0.3 %  
292 of organic carbon; we are assuming that the material left after chemical digestion was

293 mainly inorganic. This is in accordance with the fact that some organisms were deposit  
294 feeders and that they are ingesting sediment particles. The samples with the lowest  
295 digestion efficiencies corresponded to *Glandiceps talaboti* and *Notomastus* sp., which are  
296 subsurface deposit feeders. Such organisms typically process at least one body weight of  
297 sediment daily. As a consequence, their alimentary tract contains large volumes of  
298 sediment that are not eliminated during chemical digestion (Lopez and Levinton, 1987).  
299 These results underlined the importance of the weight-specific feeding rates to be  
300 considered when characterizing the plastic that is ingested by benthic species.

301 Compared to enzymatic digestion, chemical digestion offers many advantages since it is  
302 very efficient and not expensive, but a disadvantage is the possible alteration of some  
303 polymers. It was recently reported that even if PET was resistant to digestion when  
304 potassium hydroxide was used at 60 °C, smaller particles, such as PET fibers, did not resist  
305 such temperatures; thus, lower temperatures are recommended (Treilles et al., 2020). For  
306 instance, the digestion of seafood samples at 60 °C resulted in 32% recoveries for PET  
307 (Ribeiro and al. 2020). For this reason, chemical digestion was performed at 40 °C. We  
308 obtained an extraction procedure efficiency for the six spiked polymers between 82 and  
309 129%, which was within the precision margin of the MS/MS method, so we estimated that  
310 the recoveries were acceptable (Table SI 5).

### 311 **3.3. Method Validation and Performance**

312 To proceed to the fabrication of the external calibration we first cryo-milled the polymer  
313 separately. They were then mixed in an inert glass fiber matrix also previously grinded  
314 and calcined to remove any trace of polymers. The external standards were first prepared  
315 at concentrations ranging from 1 mg.g<sup>-1</sup> to 5 mg.g<sup>-1</sup> and the powder was then diluted by a  
316 factor 10. To obtain the external calibration we prepared 5 dilutions to reach the calibration  
317 range detailed Table SI 3. The repeated injection of an external standard (N=12) showed a  
318 standard deviation below 20% for all polymers considered. We thus consider the  
319 homogenization of the powders was satisfactory. The response was linear within the  
320 calibration range for each polymer with a correlation value (R<sup>2</sup>) greater than 0.85 (Table  
321 2). After digestion and filtration of the samples on glass fiber filters, the filters were cryo-  
322 ground to present good homogeneity, as only a fraction, typically 2 mg, was introduced in  
323 the pyrolysis chamber. After cryo-grinding, a sample analyzed in triplicate showed a  
324 standard deviation below 35% for all polymers considered (Table SI 6). We estimated that

325 cryo-grinding was efficient and that the sample was sufficiently homogeneous. The other  
326 samples were analyzed once.

327 The procedural and field blank polymer concentrations are presented in Table SI 4. The  
328 amount of PMMA in the samples was not determined because the concentrations in the  
329 sampling control blank were rather important (4.7  $\mu\text{g/g}$  filter, table SI 4). Further studies  
330 are needed to determine the potential source of contamination and to improve the QA/QC  
331 for this polymer.

332 The potential impact of the remaining matter after chemical digestion on the polymer  
333 analysis was assessed with the standard addition method. The pyrolytic fingerprint of all  
334 the polymers was identical when the polymers were injected as a pure sample or within the  
335 matrix, indicating that the presence or residual organic or inorganic matter did not interfere  
336 with the polymer pyrolysis or the MS/MS detection. The case of PE is remarkable because  
337 some natural organic molecules (like lipids) could thermally decompose into dienes as it  
338 was recently reported (Rauert et al., 2022). In order to ensure that the remaining matter  
339 after sample preparation did not enhance the signal of PE we used an additional validation  
340 criterion based on the recording of two indicator compounds (the analogues with 13 and  
341 14 carbon atoms). The ratios recorded and compared to the external standards are reported  
342 in Figure SI 1.

343 Table 2: Polymers targeted together with the indicator compound selection and external  
344 calibration characteristics.

<b>Polymer</b>	<b>Indicator compound</b>	<b>Quantification transition (m/z)</b>	<b>External calibration range (<math>\mu\text{g}</math>)</b>	<b>Numbers of point</b>	<b>r<sup>2</sup></b>
<b><i>PMMA</i></b>	methyl methacrylate	100>41	35 to 380 ng	6	0.98
<b><i>PP</i></b>	2,4-dimethylhept-1-ene	70>55	30 to 300 ng	5	0.90
<b><i>PE</i></b>	1,12-tridecadiene	95>67	130 to 1360 ng	6	0.88
<b><i>PET</i></b>	dimethyl terephthalate	163>135	25 to 265 ng	6	0.96
<b><i>PS</i></b>	5-hexene-1,3,5-triyltribenzene (styrenetrimer)	207>129	50 to 385 ng	5	0.99

<i>PC</i>	2,2-bis(4'-methoxy-phenyl)propane	241>133	27 to 280 ng	6	0.95
-----------	-----------------------------------	---------	--------------	---	------

345

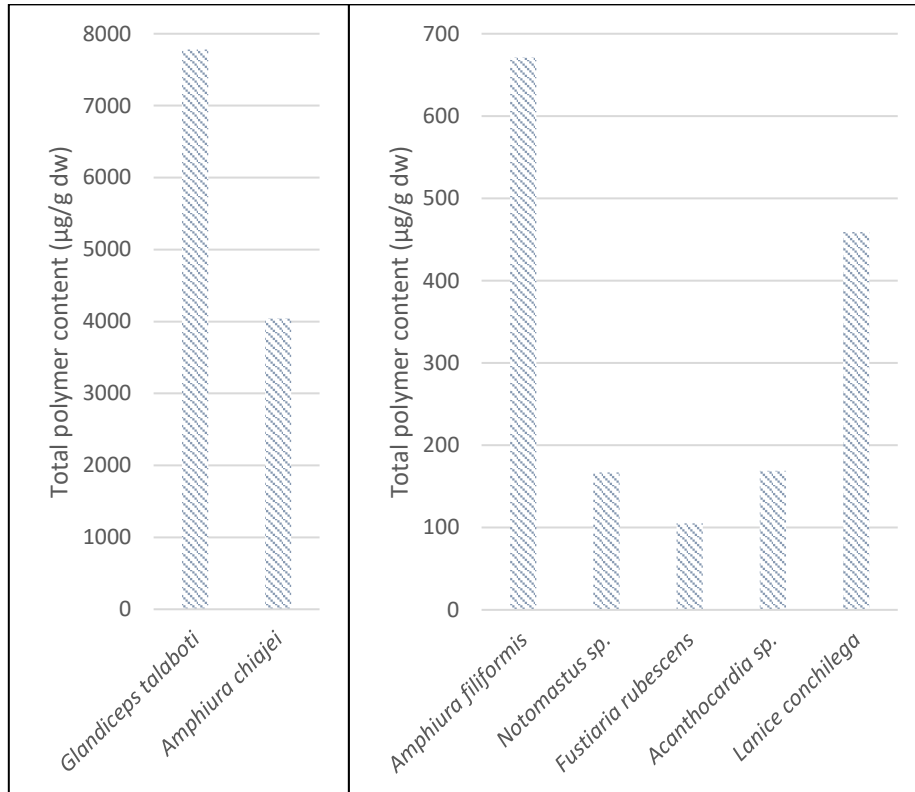
### 346 **3.4. Polymer content in the samples**

347 In general, we systematically detected plastic in the marine benthic animals analyzed. The  
 348 total polymer contents (Figure 2 and Table SI 7) varied from one specimen to another and  
 349 were between 105 and 7780 µg/g dry weight. These margins are within those recently  
 350 determined by Py-GC–MS for seafood (Ribeiro et al., 2020). There is not yet an established  
 351 pattern between the content of plastic in marine organisms and the feeding modes, marine  
 352 habitat or trophic position, even with a large sample set. Microplastic accumulation in the  
 353 marine food chain has been supported by some authors (Carbery et al., 2018), while a recent  
 354 critical review concluded that no plastic biomagnification occurred (Walkinshaw et al.,  
 355 2020). The authors argued that microplastics do not translocate from the digestive system  
 356 into tissues or into circulatory fluid and that microplastics are only transitory contaminants  
 357 with a limited residence time within organisms. Nevertheless, the mechanisms of plastic  
 358 particle ingestion, egestion or excretion are still not well understood (Cole et al., 2016). In  
 359 general, authors assume that the residence time of plastic particle in the digestive system  
 360 is deeply correlated with the particle size, shape and rugosity, which are very  
 361 heterogeneous in the environment and could explain the great variations obtained between  
 362 specimens, in addition to ecological or environmental factors.

363 In our study, we collected species with variable feeding modes. *Glandiceps talaboti*,  
 364 *Notomastus* sp. and *Amphiura chiajei* are strict deposit feeders (Buchanan, 1964), while  
 365 *Lanice conchilega* is both a suspension feeder and deposit feeder, depending on the  
 366 environmental conditions (Word, 1990; (Zarkanellas and Kattoulas, 1982). *Amphiura*  
 367 *filiformis* is known to have a main filtering activity (Buchanan, 1964). *Acanthocardia*  
 368 *paucicostata* is a strict suspension feeder, and *Fustiaria rubescens* is a carnivorous feeding  
 369 mainly on foraminifers from sediment surfaces (Gofas et al., 2011). These species are  
 370 known to be good integrators of environmental variation because of their reduced mobility.  
 371 Therefore, their plastic content may be considered a good proxy of the plastic content of  
 372 the environment in the same region, with the limit of the spatial heterogeneity of  
 373 microplastics on the sea floor. Overall, our results agreed with this hypothesis by indicating  
 374 that the type of polymer recovered from benthic animals with different feeding modes  
 375 corresponds to the distribution of the polymer in the oceans. Nonetheless we observed

376 important variation among individuals; this variability was often reported and is not yet  
377 explained (Ribeiro et al., 2020).

378  
379



380  
381  
382  
383

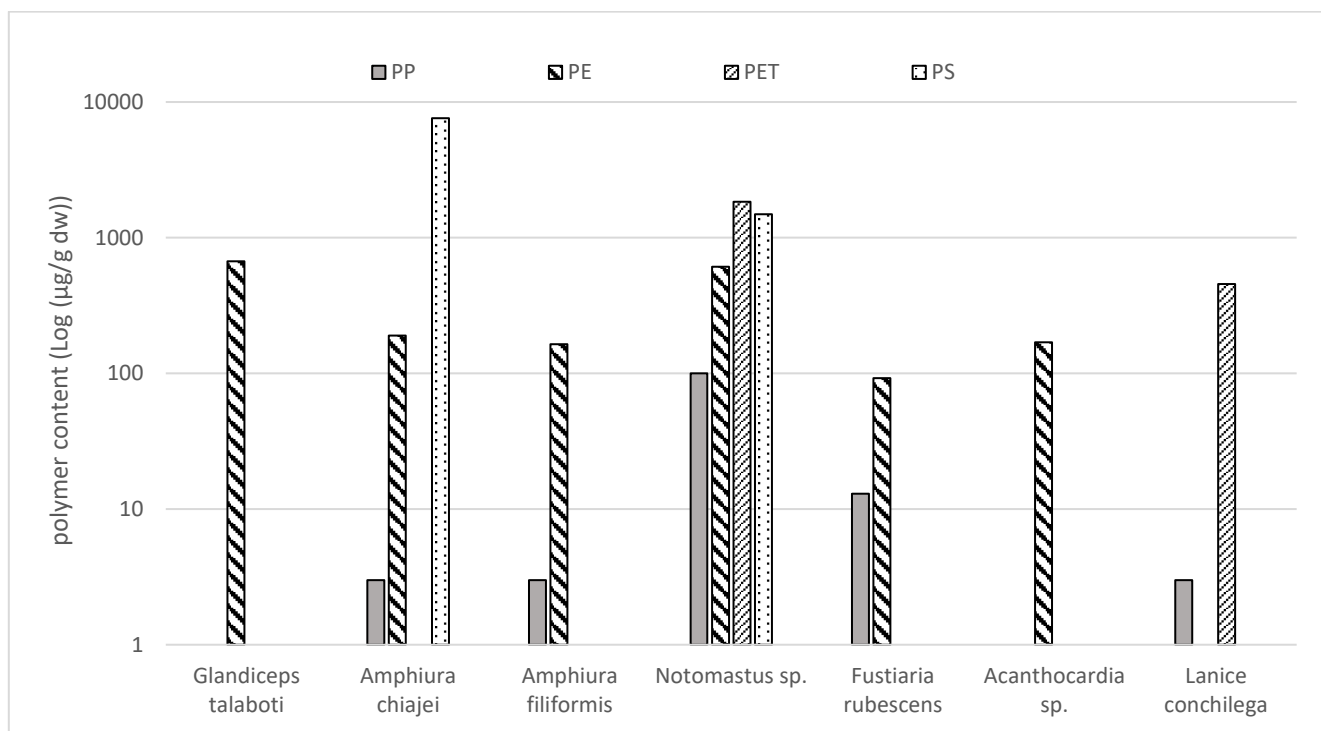
Figure 2: Total polymer content expressed in µg per gram of dry weight (µg/g dw).

384 PE was detected in six samples of the seven analyzed samples (Figure 3) at concentrations  
385 up to 670 µg/g dw for the *Glandiceps talaboti* individual. We noticed that PE was often  
386 present in the largest proportions, often superior to 80% of the total polymer content. It has  
387 been reported that PE was dominant in marine samples with an average proportion of 42%  
388 at the sea surface and with a decrease in abundance through the water column (Erni-Cassola  
389 et al., 2019). Our results agreed with those of Missawi et al., who reported that PE was  
390 dominant in the polychaete worm *Hediste diversicolor* on the Tunisian coast in the  
391 Mediterranean Sea, with important variations among individuals and sites, whereas PP was  
392 detected in lesser proportions than those of PE (Missawi et al., 2020), which is in  
393 accordance with the reported concentrations at sea (Erni-Cassola et al., 2019).

394 *Notomastus sp.* et *Lanice conchilega* presented high contents of PET, which are likely to  
395 be associated with deposit feeders because it is a polymer with a higher density than that  
396 of sea water. Previous studies using spectroscopic characterization emphasized that a high

397 proportion of PETs were detected in detritivores, which corresponds to plastic fibers (Renzi  
 398 et al., 2020). PET fibers have also been detected in high proportions in seafloor samples  
 399 (Kane et al., 2020). Figure 3 also shows that *Amphiura chiajei* and *Notomastus sp.*  
 400 exhibited a high content of PS. They are both deposit feeders and are likely exposed to  
 401 denser polymers such as PS. Along the same line, PMMA, which is also known to be more  
 402 abundant in the sediment than at its surface (Renzi et al., 2020), has not been detected in  
 403 suspension feeders such as *A. filiformis* and *A. paucicostata*. This could be explained by  
 404 the relatively high limit of detection for PMMA under our conditions.

405



406

407 Figure 3: Polymer content in the benthic individuals (expressed in µg/g dry weight).  
 408

409 **Concluding remarks**

410 The study demonstrates that a method based on Py-GC-MS/MS leads to a simplified  
 411 sample purification and enables microplastic contents down to 0.7 µm to be determined  
 412 with good reliability in organisms. Py-GC-MS does not provide information on the color,  
 413 shape, or size of microplastics and is complementary to methods that are based on  
 414 spectroscopy (Primpke et al., 2020). The use of pyrolysis to quantify microplastics still  
 415 involves limitations and areas of improvement that need to be considered before it becomes  
 416 a standardized technique. As a first glance, the use of internal standards will certainly



417 improve the precision of the measurements even if the developments in this direction  
418 present some technical difficulties (Lauschke et al., 2021) that are challenging because very  
419 few isotopic analog resins are commercially available. Other important undertakings  
420 involve achieving a better understanding of matrix interference and the effect of polymer  
421 weathering on the pyrolytic response (Ainali et al., 2021; (Biale et al., 2021; (Toapanta et  
422 al., 2021). The most appealing aspect of Py-GC–MS is that it does not have size limitations,  
423 as there is still very little known about the behavior of small microplastics in the  
424 environment and their interaction with organisms. We emphasize the promising potential  
425 for the use of Py-GC–MS as it involves straightforward sample preparation, even with  
426 complex samples, and the possibility of increasing our capacity to analyze larger sample  
427 sets for environmental assessments. To gain a better understanding of the interactions of  
428 benthic community with plastic pollution, the variation in plastic concentrations with  
429 sediment depth at different locations should be investigated, and this could be first explored  
430 by focusing on a single species with a strict feeding mode.

431

432

Supporting material

433

434

435 **Determination of the microplastic content in Mediterranean benthic**  
436 **organisms by pyrolysis-gas chromatography-tandem mass**  
437 **spectrometry**

438 Magali Albignac<sup>1</sup>, Jean François Ghiglione<sup>2</sup>, Céline Labrune<sup>3</sup>, Alexandra ter Halle<sup>1\*</sup>

439 <sup>1</sup>CNRS, Université de Toulouse, Laboratoire des Interactions Moléculaires et Réactivité Chimique  
440 et Photochimique (IMRCP), UMR 5623, Toulouse, France

441 <sup>2</sup>CNRS, Sorbonne Université, Laboratoire d'Océanographie Microbienne (LOMIC), UMR 7621,  
442 Observatoire Océanologique de Banyuls, Banyuls sur mer, France

443 <sup>3</sup>CNRS, Sorbonne Université, Laboratoire d'Ecogéochimie des Environnements Benthiques  
444 (LECOB), UMR 8222, Observatoire Océanologique de Banyuls, Banyuls sur mer, France

445

446 **Table SI1:** Optimized conditions for Pyrolysis-GCMS/MS

447

---

**Pyrolyzer**

Carrier gas helium

Pyrolysis temperature 600°C

Pyrolysis time 30 s

**Gas chromatogram**

Initial temperature 40°C

Flow 1.25 mL.min<sup>-1</sup>

Temperature program 40°C (2 min) => 300°C (5 min) at 10°C.min<sup>-1</sup>

Transfer line temperature 280°C

**Mass spectrometer**

Mode Multiple Reaction Monitoring

Scan time 0.15 s

Source temperature 300°C

---

448

449 Table SI 2: Additional information for polymer detection and quantification after MS/MS  
 450 development.  
 451

<b>Indicator compound</b>	<b>Retention time</b>	<b>Quantification transition (Tq)</b>	<b>Confirmation transition (Tc)</b>	<b>Tc/Tq (%)*</b>
<i>Methyl-methacrylate</i>	2.73	100>41 (15eV)	100>69 (10eV)	76.1
<i>Dimethyle-heptene</i>	4.47	70>55 (10 eV)	126>83 (5 eV)	13.9
<i>1,12 tridecadiene</i>	11.36	95>67 (10 eV)	109>67 (10 eV)	43.1
<i>Dimethylterephthalate</i>	14.33	163>135 (10 eV)	163>103 (15 eV)	69.9
<i>StyreneTrimere</i>	23.4	207>129 (10 eV)	207>91 (15 eV)	46.7
<i>Methyl-bis-phenol A</i>	20.26	241>133 (15 eV)	256>241 (10 eV)	81.3

452  
 453 \*The ratio Tc/Tq was determined over the first 3 most concentrated external standards  
 454 injected for the calibration  
 455 \*\* Typically, we introduce 2 mg of standard or sample for pyrolysis analysis  
 456

457 **Table SI 3:** External standards amount injected range and MS/MS peak intensity.

---

<b>Polymer</b>	<b>Range of concentration of the 6 calibration points (ng)</b>	<b>Range of corresponding peak area for the transition of quantification</b>
PMMA	37 - 384	1E+05 - 2E+06
PP	30 - 309	1E+05 - 8E+05
PE	133 - 1357	8E+03 - 9E+04
PET	26 - 264	6E+04 - 3E+06
PC	50 - 508	7E+04 - 1E+06
PS	27 - 280	1E+06 - 2E+07

---

458

459 Table SI 4: Amount of polymer detected in the sampling control and the procedural control.

<b>Polymer targeted</b>	<b>Sampling control blank</b>	<b>Procedural control</b>
<i>PMMA</i> ( $\mu\text{g/g}$ )	4.7	2.7
<i>PP</i> ( $\mu\text{g/g}$ )	n.d	n.d.
<i>PE</i> ( $\mu\text{g/g}$ )	n.d	n.d.
<i>PET</i> ( $\mu\text{g/g}$ )	40.0	0.8
<i>PS</i> ( $\mu\text{g/g}$ )	4.0	0.7
<i>PC</i> ( $\mu\text{g/g}$ )	n.d	n.d.

460  
461  
462  
463  
464

n.d.: not determined. The indicator compound peak was not detected, and the Tq/Tc ratio was not confirmed.

465 Table SI 5: Digestion recoveries for the polymers with the standard addition method

<b>Polymer targeted</b>	<b>Concentrations of the polymer in the inert matrix (<math>\mu\text{g}\cdot\text{g}^{-1}</math>)</b>	<b>Amount of polymer added for the recovery test (ng)</b>	<b>Proportion of polymer recovered after chemical digestion (%)</b>
<i>PMMA</i>	607	6182	107
<i>PP</i>	489	4978	82
<i>PE</i>	2147	4260	111
<i>PET</i>	418	4513	129
<i>PS</i>	804	8196	122
<i>PC</i>	443	9036	116

466

467

468 Table SI 6: The *Lanice conchilega* sample was analyzed in triplicate. The relative  
469 standard deviations were reported for all polymers and did not exceed 35%.

470

---

<b>Polymer targeted</b>	<b>Indicator compound</b>	<b>SD - %</b>
<i>PMMA</i>	Methyl-methacrylate	19
<i>PP</i>	Dimethyle-heptene	23
<i>PE</i>	1,12 tridecadiene	24
<i>PET</i>	Dimethylterephthalate	29
<i>PS</i>	StyreneTrimere	34
<i>PC</i>	Methyl-bis-phenol A	10

---

471

472



473 Table SI 7: Concentration of the polymer targeted expressed in  $\mu\text{g}$  per gram of dry wet  
 474 ( $\mu\text{g/g}$  dw). The results are presented with a standard deviation of 35%.

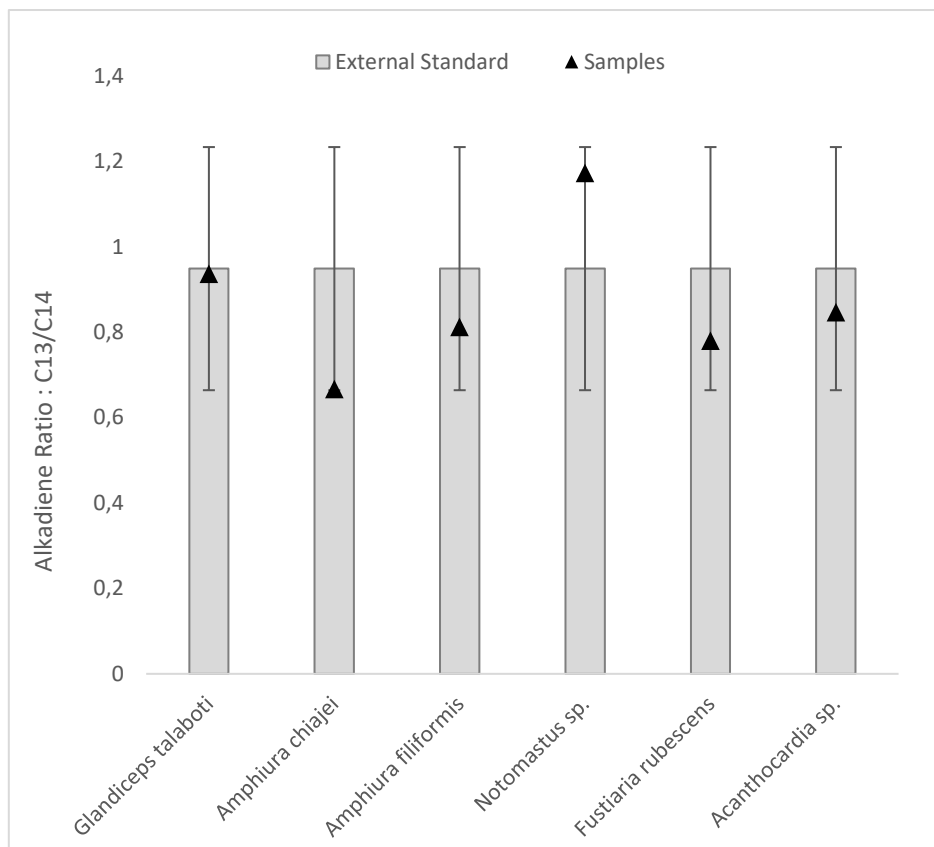
475

Sample N°	2	3	4	5	6	7	8
	<b>Glandiceps talaboti</b>	<b>Amphiura chiajei</b>	<b>Amphiura filiformis</b>	<b>Notomastus sp.</b>	<b>Fustiaria rubescens</b>	<b>Acanthocardia sp.</b>	<b>Lanice conchilega</b>
<b><i>PMMA</i></b> <b>(<math>\mu\text{g/g}</math>)</b>	n.d.	n.d.	n.d.	n.d.	n.d.	n.d.	n.d.
<b><i>PP</i></b> <b>(<math>\mu\text{g/g}</math>)</b>	1	3	3	100	13	n.d.	3
<b><i>PE</i></b> <b>(<math>\mu\text{g/g}</math>)</b>	670	190	164	610	92	169	n.d.
<b><i>PET</i></b> <b>(<math>\mu\text{g/g}</math>)</b>	n.d.	n.d.	n.d.	1845	n.d.	n.d.	456
<b><i>PS</i></b> <b>(<math>\mu\text{g/g}</math>)</b>	n.d.	7587	n.d.	1487	n.d.	n.d.	n.d.
<b><i>PC</i></b> <b>(<math>\mu\text{g/g}</math>)</b>	n.d.	n.d.	n.d.	23	n.d.	n.d.	n.d.

476

477 n.d.: the concentrations were not determined.

478



479

480 Figure SI 1 : Ratio of the peak areas for the two indicator compounds selected to monitor  
 481 PE: the alkadienes congeners with 13 and 14 carbons atoms. The grey bars represent the  
 482 mean values calculated for the external standards (within the calibration range presented)  
 483 and the black triangles represent the values obtained for the samples. The error bars set at  
 484 30% represent the validation criterion adopted to ensure that PE quantification exclude  
 485 the signal of natural organic matter.

486

487  
488  
489  
490  
491  
492  
493  
494  
495  
496  
497  
498  
499  
500  
501  
502  
503  
504  
505  
506  
507  
508  
509  
510  
511  
512  
513  
514  
515  
516  
517  
518  
519  
520  
521  
522  
523  
524  
525  
526  
527  
528  
529  
530  
531  
532  
533  
534  
535  
536  
537  
538

## References

- Ainali, N.M., et al., 2021. Aging effects on low- and high-density polyethylene, polypropylene and polystyrene under UV irradiation: An insight into decomposition mechanism by Py-GC/MS for microplastic analysis. *Journal of Analytical and Applied Pyrolysis* 158. <https://doi.org/10.1016/j.jaap.2021.105207>.
- Anastasopoulou, A., et al., 2013. Plastic debris ingested by deep-water fish of the Ionian Sea (Eastern Mediterranean). *Deep-Sea Research Part I-Oceanographic Research Papers* 74, 11-13. <https://doi.org/10.1016/j.dsr.2012.12.008>.
- Angiolillo, M., et al., 2021. Distribution of seafloor litter and its interaction with benthic organisms in deep waters of the Ligurian Sea (Northwestern Mediterranean). *Sci. Total Environ.* 788. <https://doi.org/10.1016/j.scitotenv.2021.147745>.
- Biale, G., et al., 2021. A Systematic Study on the Degradation Products Generated from Artificially Aged Microplastics. *Polymers* 13. <https://doi.org/10.3390/polym13121997>.
- Buchanan, J.B., 1964. A comparative study of some features of the biology of *Amphiura filiformis* and *Amphiura chiajei* (Ophiuroidea) considered in relation to their distribution. *J Mar Biol Ass UK* 44, 615-624.
- Carbery, M., et al., 2018. Trophic transfer of microplastics and mixed contaminants in the marine food web and implications for human health. *Environ Int* 115, 400-409. <https://doi.org/10.1016/j.envint.2018.03.007>.
- Cole, M., et al., 2016. Microplastics Alter the Properties and Sinking Rates of Zooplankton Faecal Pellets. *Environ. Sci. Technol.* 50, 3239-3246. <https://doi.org/10.1021/acs.est.5b05905>.
- Coll, M., et al., 2010. The Biodiversity of the Mediterranean Sea: Estimates, Patterns, and Threats. *Plos One* 5. <https://doi.org/10.1371/journal.pone.0011842>.
- Conslì, P., et al., 2020. Characterization of seafloor litter on Mediterranean shallow coastal waters: Evidence from Dive Against Debris (R), a citizen science monitoring approach. *Marine Pollution Bulletin* 150. <https://doi.org/10.1016/j.marpolbul.2019.110763>.
- Danovaro, R., et al., 2020. Towards a marine strategy for the deep Mediterranean Sea: Analysis of current ecological status. *Marine Policy* 112. <https://doi.org/10.1016/j.marpol.2019.103781>.
- de Madron, X.D., et al., 2017. Deep sediment resuspension and thick nepheloid layer generation by open-ocean convection. *J Geophys Res-Oceans* 122, 2291-2318. <https://doi.org/10.1002/2016jc012062>.
- Dehaut, A., et al., 2016. Microplastics in seafood: Benchmark protocol for their extraction and characterization. *Environ. Pollut.* 215, 223-233. <https://doi.org/10.1016/j.envpol.2016.05.018>.
- Dierkes, G., et al., 2019. Quantification of microplastics in environmental samples via pressurized liquid extraction and pyrolysis-gas chromatography. *Anal Bioanal Chem* 411, 6959-6968. <https://doi.org/10.1007/s00216-019-02066-9>.
- Erni-Cassola, G., et al., 2019. Distribution of plastic polymer types in the marine environment; A meta-analysis. *J. Hazard. Mater.* 369, 691-698. <https://doi.org/10.1016/j.jhazmat.2019.02.067>.
- Fischer, M., Scholz-Bottcher, B.M., 2017. Simultaneous Trace Identification and Quantification of Common Types of Microplastics in Environmental Samples by Pyrolysis-Gas Chromatography-Mass Spectrometry. *Environ. Sci. Technol.* 51, 5052-5060. <https://doi.org/10.1021/acs.est.6b06362>.
- Galgani, F., et al., 2000. Litter on the sea floor along European coasts. *Marine Pollution Bulletin* 40, 516-527. [https://doi.org/10.1016/s0025-326x\(99\)00234-9](https://doi.org/10.1016/s0025-326x(99)00234-9).
- Galgani, F., et al., 1996. Accumulation of debris on the deep sea floor off the French Mediterranean coast. *Mar Ecol Prog Ser* 142, 225-234. <https://doi.org/10.3354/meps142225>.
- Galloway, T.S., et al., 2017. Interactions of microplastic debris throughout the marine ecosystem. *Nat Ecol Evol* 1. <https://doi.org/10.1038/s41559-017-0116>.
- Ghiglione, J.F., Laudet, V., 2020. Marine Life Cycle: A Polluted Terra Incognita Is Unveiled. *Current Biology* 30, R130-R133. <https://doi.org/10.1016/j.cub.2019.11.083>.
- Gofas, S., et al. (2011) *Moluscos marinos de Andalucía*.

539 Hall, S.J., 2002. The continental shelf benthic ecosystem: current status, agents for change and  
540 future prospects. *Environmental Conservation* 29, 350-374.  
541 <https://doi.org/10.1017/s0376892902000243>.

542 Hermsen, E., et al., 2018. Quality Criteria for the Analysis of Microplastic in Biota Samples: A  
543 Critical Review. *Environ. Sci. Technol.* 52, 10230-10240. <https://doi.org/10.1021/acs.est.8b01611>.

544 Kane, I.A., et al., 2020. Seafloor microplastic hotspots controlled by deep-sea circulation. *Science*  
545 368, 1140-+. <https://doi.org/10.1126/science.aba5899>.

546 Kooi, M., et al., 2017. Ups and Downs in the Ocean: Effects of Biofouling on Vertical Transport of  
547 Microplastics. *Environ. Sci. Technol.* 51, 7963-7971. <https://doi.org/10.1021/acs.est.6b04702>.

548 Lauschke, T., et al., 2021. Evaluation of poly(styrene-d5) and poly(4-fluorostyrene) as internal  
549 standards for microplastics quantification by thermoanalytical methods. *Journal of Analytical and*  
550 *Applied Pyrolysis* 159. <https://doi.org/10.1016/j.jaap.2021.105310>.

551 Lopez, G.R., Levinton, J.S., 1987. Ecology of deposit-feeding animals in marine-sediments.  
552 *Quarterly Review of Biology* 62, 235-260. <https://doi.org/10.1086/415511>.

553 Manea, E., et al., 2020. Towards an Ecosystem-Based Marine Spatial Planning in the deep  
554 Mediterranean Sea. *Sci. Total Environ.* 715. <https://doi.org/10.1016/j.scitotenv.2020.136884>.

555 Missawi, O., et al., 2020. Abundance and distribution of small microplastics ( $\leq 3 \mu\text{m}$ ) in  
556 sediments and seaworms from the Southern Mediterranean coasts and characterisation of their  
557 potential harmful effects. *Environ. Pollut.* 263. <https://doi.org/10.1016/j.envpol.2020.114634>.

558 Okoffo, E.D., et al., 2020. Identification and quantification of selected plastics in biosolids by  
559 pressurized liquid extraction combined with double-shot pyrolysis gas chromatography-mass  
560 spectrometry. *Sci. Total Environ.* 715. <https://doi.org/ARTN> 136924  
561 10.1016/j.scitotenv.2020.136924.

562 Pico, Y., Barcelo, D., 2020. Pyrolysis gas chromatography-mass spectrometry in environmental  
563 analysis: Focus on organic matter and microplastics. *Trac-Trend Anal Chem* 130.  
564 <https://doi.org/ARTN> 115964 10.1016/j.trac.2020.115964.

565 Primpke, S., et al., 2020. Comparison of pyrolysis gas chromatography/mass spectrometry and  
566 hyperspectral FTIR imaging spectroscopy for the analysis of microplastics. *Anal Bioanal Chem* 412,  
567 8283-8298. <https://doi.org/10.1007/s00216-020-02979-w>.

568 Rauert, C., et al., 2022. Extraction and Pyrolysis-GC-MS analysis of polyethylene in samples with  
569 medium to high lipid content. *Journal of Environmental Exposure Assessment* 1, 13.  
570 <https://doi.org/10.20517/jeea.2022.04>.

571 Renzi, M., et al., 2020. Chemical composition of microplastic in sediments and protected  
572 detritivores from different marine habitats (Salina Island). *Marine Pollution Bulletin* 152.  
573 <https://doi.org/10.1016/j.marpolbul.2020.110918>.

574 Ribeiro, F., et al., 2020. Quantitative Analysis of Selected Plastics in High-Commercial-Value  
575 Australian Seafood by Pyrolysis Gas Chromatography Mass Spectrometry (vol 54, pg 9408, 2020).  
576 *Environ. Sci. Technol.* 54, 13364-13364. <https://doi.org/10.1021/acs.est.0c05885>.

577 Scholz-Bottcher, B.M., et al., 2013. An 18th century medication "Mumia vera aegyptica" - Fake or  
578 authentic? *Organic Geochemistry* 65, 1-18. <https://doi.org/10.1016/j.orggeochem.2013.09.011>.

579 Schwaferts, C., et al., 2019. Methods for the analysis of submicrometer- and nanoplastic particles  
580 in the environment. *Trends Anal. Chem.* 112, 52-65. <https://doi.org/10.1016/j.trac.2018.12.014>.

581 Sojak, L., et al., 2007. High resolution gas chromatographic-mass spectrometric analysis of  
582 polyethylene and polypropylene thermal cracking products. *Journal of Analytical and Applied*  
583 *Pyrolysis* 78, 387-399. <https://doi.org/10.1016/j.jaap.2006.09.012>.

584 Toapanta, T., et al., 2021. Influence of surface oxidation on the quantification of polypropylene  
585 microplastics by pyrolysis gas chromatography mass spectrometry. *Sci. Total Environ.* 796.  
586 <https://doi.org/10.1016/j.scitotenv.2021.148835>.

587 Treilles, R., et al., 2020. Impacts of organic matter digestion protocols on synthetic, artificial and  
588 natural raw fibers. *Sci. Total Environ.* 748. <https://doi.org/ARTN> 141230  
589 10.1016/j.scitotenv.2020.141230.

590 Tubau, X., et al., 2015. Marine litter on the floor of deep submarine canyons of the Northwestern  
591 Mediterranean Sea: The role of hydrodynamic processes. *Prog Oceanogr* 134, 379-403.  
592 <https://doi.org/10.1016/j.pocean.2015.03.013>.

593 Valente, T., et al., 2020. Macro-litter ingestion in deep-water habitats: is an underestimation  
594 occurring? *Environmental Research* 186. <https://doi.org/10.1016/j.envres.2020.109556>.

595 Walkinshaw, C., et al., 2020. Microplastics and seafood: lower trophic organisms at highest risk of  
596 contamination. *Ecotoxicology and Environmental Safety* 190.  
597 <https://doi.org/10.1016/j.ecoenv.2019.110066>.

598 Word, J.Q., 1990. The infaunal trophic index, a functional approach to benthic community  
599 analyses.

600 Yakovenko, N., et al., 2020. Emerging use thermo-analytical method coupled with mass  
601 spectrometry for the quantification of micro(nano)plastics in environmental samples. *TrAC Trends*  
602 *in Analytical Chemistry* 131, 115979. <https://doi.org/https://doi.org/10.1016/j.trac.2020.115979>.

603 Zarkanellas, A.J., Kattoulas, M.E., 1982. The Ecology of Benthos in the Gulf of ThermaTkos, Greece.  
604 *Marine Ecology* 3, 21-39.

605 Zhou, X.X., et al., 2019. Cloud-Point Extraction Combined with Thermal Degradation for  
606 Nanoplastic Analysis Using Pyrolysis Gas Chromatography-Mass Spectrometry. *Analytical*  
607 *Chemistry* 91, 1785-1790. <https://doi.org/10.1021/acs.analchem.8b04729>.

608

609